Deuteron-Proton Scattering at 10.0 Mev by a Coincidence Method*

H. J. KARR,† R. O. BONDELID,† AND K. B. MATHER‡
Physics Department, Washington University, St. Louis, Missouri
(Received July 3, 1950)

A description is given of a scattering chamber possessing several novel features. This chamber was applied to the determination of absolute cross sections for elastic scattering of 10.0-Mev deuterons by protons, over a range of angles from 45° to 160° in the center-of-mass system. Two independently movable proportional counters were connected in coincidence and set at appropriate angles with respect to the incident beam so that coincidences were recorded between deuterons entering one counter and their recoil protons entering the other. The advantages and disadvantages of this system are made clear. The scattering media were thin Nylon and polyethylene-terephthalate foils. The relative cross sections reported here are believed to be accurate to ±3.5 percent and the absolute values to ±5 percent. Some comparison is made with the *mhbw* theory of Buckingham and Massey. Agreement is excellent over a considerable range of angles; but the theoretical curve is shallower than the experimental, and considerable anomaly appears at large angles. The experimental curve rises very steeply beyond about 120° in the center-of-mass system.

I. INTRODUCTION

THIS is the first of a series of articles reporting experiments on the scattering of charged nuclear particles. The scattering project at Washington University was commenced early in 1947 and entailed the construction of two independent scattering chambers, (1) detecting both scattered and recoil particles with proportional counters connected in coincidence,[1] (2) using photographic plates[2] to record tracks of scattered particles. The present article describes the coincidence chamber and auxiliary equipment together with the complete results obtained on the scattering of 10-Mev deuterons by protons. *P-d* scattering has been examined previously at 830 kev,[3] at 200–300 kev,[4] at 4.2 Mev[5] and very extensively and accurately at a set of energies from 1.5–3.5 Mev.[6] The present work extends *p-d* scattering to 5.0 Mev. The experiment was carried out as *d-p* at 10 Mev, which is equivalent to *p-d* at 5 Mev.

II. METHOD

The coincidence technique consisted in counting the number of electrical coincidences between two proportional counters which were set at such angles with respect to each other and to the incident beam that each scattered particle entering one counter resulted in the recoil particle *from the same collision* entering the other counter. One of the collision particles entered a proportional counter through a small slit, the size of which determined the counting rate and angular resolution. Its dimensions therefore had to be known accurately. It will be referred to as the *defining slit* and that counter as the *defining counter*. In *d-p* scattering either the deuterons or protons may be defined, but for consistency in this section reference will always be to the case of deuteron definition.

Associated with every scattered deuteron in the *d-p* scattering process there is a recoil proton referred to here as the conjugate proton. Moreover, there is a definite angular relationship between the path of an incident deuteron, a scattered deuteron, and a conjugate proton (Sec. III). In order to record a coincidence for every deuteron that entered the defining counter, it was imperative that every conjugate proton should enter the other counter. The *conjugate slit* had to be large enough to permit this entrance. It was merely a problem of geometry to calculate the conjugate paths of protons corresponding to every conceivable path by which a deuteron could enter the defining slit. The contour at the conjugate counter which would embrace all of these paths will be called the "geometrical conjugate pattern." The conjugate slit had to be larger than this pattern by a safety factor to allow for slight imperfections of machining and alignment, etc., and also because a certain "magnification" of the pattern

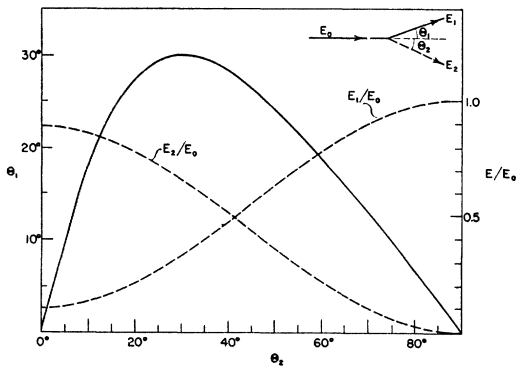

FIG. 1. Angle of deuteron scattering, Θ_1, *versus* angle of proton recoil, Θ_2, in laboratory coordinates. Also, variation of relative energy of deuteron, E_1/E_0, and of proton, E_2/E_0, with Θ_2.

* Assisted by the joint program of the ONR and the AEC.
† Now at Los Alamos, New Mexico.
‡ Now at Birmingham University, Birmingham, England.
[1] R. R. Wilson and E. C. Creutz published the first scattering data obtained by this technique (*p-p* scattering), Phys. Rev. **59**, 916 (1940); also Phys. Rev. **71**, 339 (1947), and subsequent papers.
[2] To be published.
[3] Tuve, Heydenberg, and Hafstad, Phys. Rev. **50**, 806 (1936).
[4] R. F. Taschek, Phys. Rev. **61**, 13 (1942).
[5] Heitler, May, and Powell, Proc. Roy. Soc. **190A**, 180 (1947).
[6] Sherr, Blair, Kratz, Bailey, and Taschek, Phys. Rev. **72**, 662 (1947).

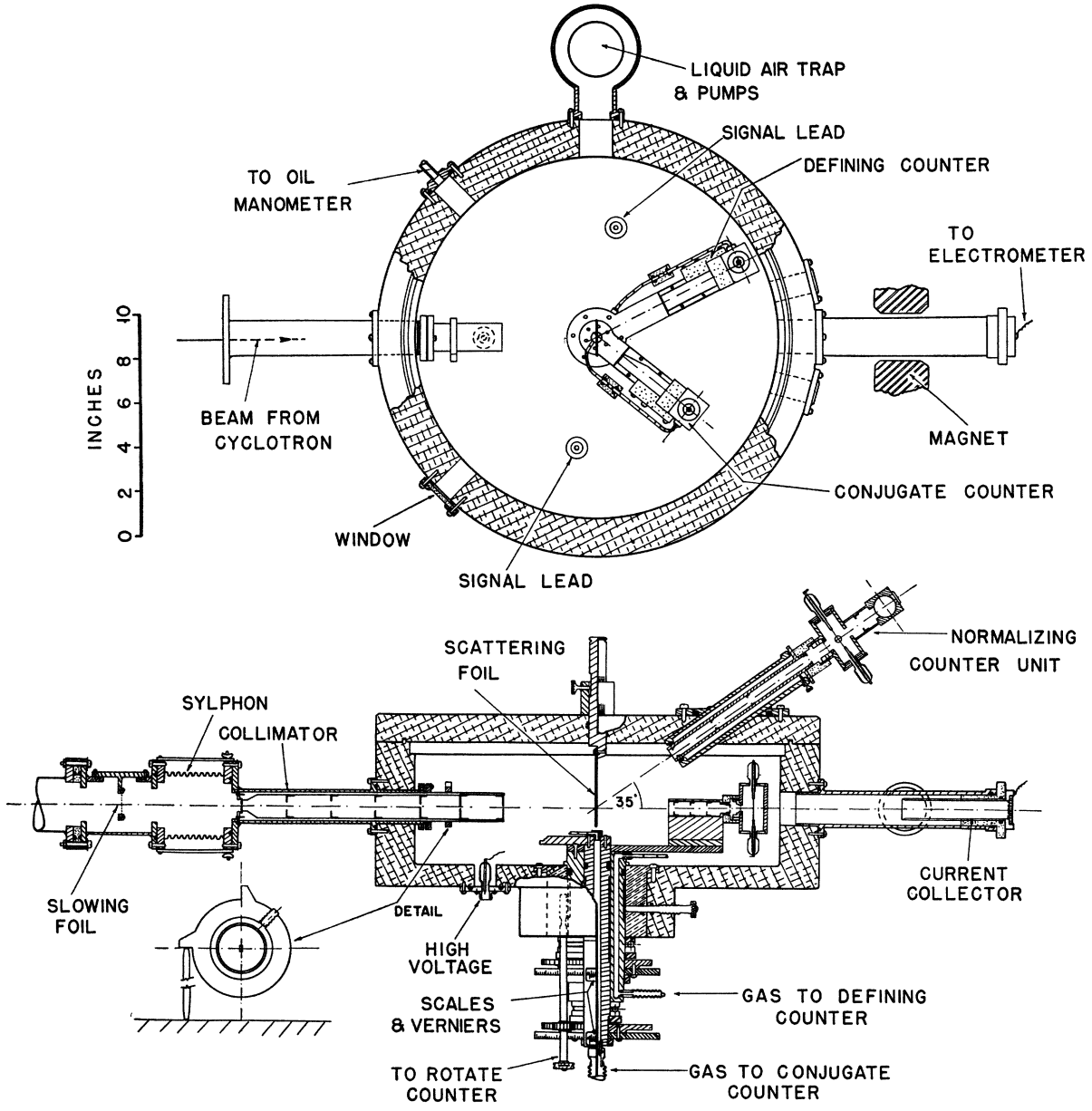

FIG. 2. Plan and side elevation of coincidence scattering chamber.

of the conjugate beam occurred owing to multiple scattering. Calculation of the geometrical conjugate pattern and its modification by multiple scattering will be outlined in Appendices I and II respectively.

III. GENERAL SCATTERING RELATIONS

If a mass, m_1, is elastically scattered through an angle, Θ_1, in the laboratory system by a mass, m_2, which recoils at an angle, Θ_2, then in non-relativistic mechanics

$$m_1/m_2=\sin(2\Theta_2+\Theta_1)/\sin\Theta_1,$$

or

$$\tan\Theta_1=\sin 2\Theta_2/[(m_1/m_2)-\cos 2\Theta_2].$$

Θ_1 is graphed against Θ_2 in Fig. 1. For a given mass ratio a specification of Θ_2 uniquely determines Θ_1. If E_0 is the energy of m_1 before collision, E_1, its energy after collision, and E_2, the recoil energy of m_2, then

$$E_2=4E_0m_1m_2\cos^2\Theta_2/(m_1+m_2)^2=(8/9)E_0\cos^2\Theta_2,$$
$$E_1=E_0-E_2=E_0\{1-(m_1/m_2)[\sin\Theta_1/\sin(\Theta_2+\Theta_1)]^2\}.$$

Calculations show that for 10-Mev deuterons ($\beta\sim 0.1$) the relativistic correction to these equations is very small. Its effect was taken into account in reconciling deuteron-defined with proton-defined data.

IV. DESCRIPTION OF THE APPARATUS

A. Cyclotron and Slit System

The source of deuterons was the Washington University 45-inch cyclotron. The primary beam had considerable energy spread at the target chamber, probably about 1 Mev. However, in the scattering experiment a narrow strip of the beam was extracted by a 5-mm slit at the target chamber. The particles passing through this slit in the correct direction could pass down a $2\frac{1}{2}$-inch tube made in several sections connected by sylphons, the whole being about 270 cm long. The fringing field of the cyclotron dispersed the beam into curved trajectories of slightly different radii of curvature, the tube being curved to accommodate the deflection which totalled approximately 9°. At the far end of the tube a portion of the dispersed beam was selected by a second slit. A small section of this beam then entered the collimator of the scattering chamber. The slit system described served the dual purpose of providing a very well collimated beam and of rendering the beam reasonably monoenergetic (~1 percent).

B. Slowing Foil and Sylphon

A brass box and sylphon were inserted between the last tube section of the slit system and the flange of the collimator. The box mounted a ring to which aluminum foils could be clamped. This arrangement was for slowing the 10-Mev beam for the study of scattering at lower energies (not reported here). The sylphon served as a flexible connector for aligning the chamber with the beam.

C. Collimator

A semi-schematic illustration of the scattering chamber[7] is shown in Fig. 2. The collimator comprised two concentric brass tubes, the inner of which could slide and rotate in the outer. The inner tube mounted two defining slits (the first and next to last in Fig. 2) 10.0 inches apart. The other slits in the collimator were essentially baffles intended to reduce the effect of slit scattering which occurred at the edges of both defining slits. The most important baffle was the last one, which controlled the size of the cone of particles which sprayed from the second defining slit. For the collimator arrangement of the December and April runs the maximum angle of spray[8] measured from the axis of the beam was about 3°.

The collimator and defining slits used for the December and April runs were rectangular[9] in shape and for the September run they were circular.

The dimensions of the beam at the scattering foil entered into calculations of the geometrical conjugate pattern and in application of a correction, if necessary, for loss of counts when the conjugate slit size was inadequate. It was difficult to calculate the cross section of the beam at the scattering foil because of uncertainty as to the state of collimation of the particles reaching the chamber from the cyclotron. As this was important, it was measured. A photographic plate of the Nuclear Research kind was placed at the center of the chamber in the normal position of the foil. A very short exposure was given with the cyclotron, and the plate was withdrawn, developed, and scanned. The numbers of deuteron tracks per unit area were counted over the area of exposure. This observation established the beam pattern including penumbra effects. The maximum dimensions were 0.110 cm×0.241 cm. The dimensions of the collimator slits were 0.103 cm×0.208 cm.

The collimator slits had one dimension considerably greater than the other for a purpose. At certain angles the height of the beam had to be small while the width was relatively unimportant, and *vice versa* at some other angles. Hence, by rotation of the collimator through 90° the more favorable condition for the pair of angles being studied was available. A device was attached to the collimator to assist in making this change accurately (see detail, Fig. 2). It consisted of a ring with two projecting teeth whose faces were on perpendicular diameters of the ring. This was fastened to the inner tube of the collimator so that when one face was horizontal the slit was horizontal also. To facilitate

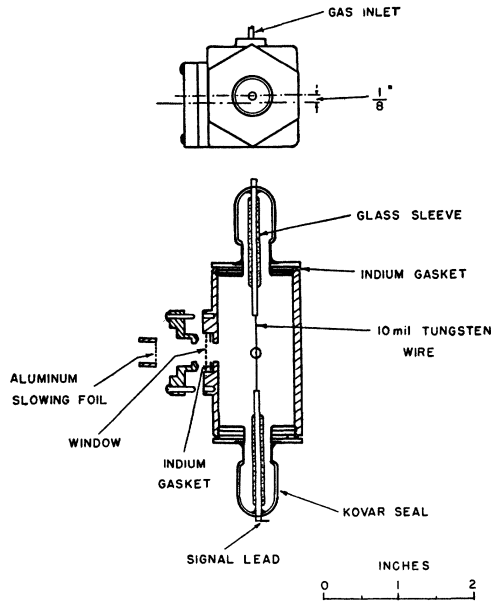

FIG. 3. Schematic of proportional counter, and mount for slowing foils.

[7] Our design was influenced to some extent by the Los Alamos scattering chamber, the details of which were made available to us late in 1946.

[8] This observation considers single scattering only. Particles can be doubly scattered and emerge with virtually any angle less than 90°.

[9] From the considerations of Appendix I it can be seen that the conjugate slit size and shape are dependent on the size and shape of the collimator and defining slits. For a given counting rate (i.e., solid angle $d\Omega$) the rectangular slits permit a more efficient use of the available conjugate area.

setting either face horizontal a post was machined to a length equal to the height of the axis of the collimator from the floor of the chamber.

D. Chamber

The chamber was turned from a solid aluminum forging. The external diameter was 20 inches, internal diameter 16.5 inches, and internal depth 5.5 inches. The lid was located by a tongue and groove and sealed with a rubber gasket. Seven holes were bored in the cylindrical wall of the chamber for attachment of various devices needed or potentially needed. High precision was demanded in the machining of the chamber. In particular, the axis of the collimator had to intersect and be perpendicular to the axis of rotation of the counters. The tolerance on this was ± 0.001 inch.

E. Current Collector

After traversing the chamber the beam was collected by a Faraday cup insulated from the supporting tube by a polystyrene ring. The far end of the cup was covered by nickel gauze and a glass disk painted with a mixture of willemite and clear Glyptal. The painted glass fluoresced under bombardment and aided alignment of the chamber. The Faraday cup was connected by a coaxial line to the integrator (Sec. VI). A permanent magnet ($\sim$500 gauss) was mounted over the current collector to avoid errors in charge measurement from secondary electron effects. (Apparently any effect was negligible, since removing the magnet did not affect the rate of integration.)

F. Proportional Counters and Their Mechanical Movement

Figure 3 shows one of the counters. The internal dimensions of both counters were made the same so that they would have the same operating characteristics. They were machined from solid brass blocks to an inside diameter of 1.0 inch. A center wire of 10-mil tungsten was supported by Kovar-to-glass seals soldered to the ends of the counter. The active region was limited to about one inch by the Kovar tubing projecting into the counter from each seal. Surrounding each tube was a glass sleeve to reduce the likelihood of discharge between the tube and the top of the counter. (It was found that if a discharge did occur, the counters became hypersensitive to gamma-rays and the enormous increase in background made operation impossible. When this happened, the inside of the counter was repolished and the seals and center wire were renewed.)

The window size was not the same in the two counters, the conjugate necessarily having the larger. Aluminum, Formvar, Nylon, and polyethylene-terephthalate (referred to subsequently as p.e.t.) windows were used at various times; but the p.e.t. proved most reliable. As the conjugate counter window was 0.55 inch in diameter and the counter pressure about 20 cm Hg, the window material required considerable tensile strength. P.e.t., initially 0.25 mil thick, was stretched to about 0.1 mil for the defining counter and to about 0.2 mil for the conjugate. (Neither figure was known accurately.) Gas-tight windows were obtained by sealing the p.e.t. between indium gaskets. Provision was made for the insertion of aluminum slowing foils in front of the windows. A number of small cylinders were prepared, each mounting an aluminum foil of known thickness (see Fig. 3). These could be plugged into the counter aperture so that the foil was close to the window. The counters operated at about 20 cm pressure with a mixture of argon and 5 percent CO_2. The counters were pumped and refilled several times per 24 hours. The walls of the counters were at high potential (-1000 v) and the center wire at signal level. With this system, disturbances produced by high voltage leakage in cables and decoupling condensers were minimized, since the high voltage circuit was connected to the amplifier input only via the small interelectrode capacitance of the counter. Also, this system permitted direct coupling of the center wire to the amplifier grid input without a coupling condenser. High potential and signal leads to the counters were brought into the chamber via Kovar seals through three ports in the bottom (Fig. 2). Within the chamber, flexible insulated leads connected these Kovar seals to the counters. The flexible leads proved highly satisfactory.

A slit system was set into a brass block in front of each counter. Only the defining slit immediately in front of the defining counter was critical. The area, ΔA, of this slit, together with its distance, R, from the center of the scattering foil, determined the solid angle $\Delta\Omega = \Delta A/R^2$ to which the counting rate was directly proportional. The shape of the defining slit had to be determined by the same considerations that applied to the collimator slits. At certain angles it was necessary to have a small slit height, while at other angles the slit width had to be curtailed (Appendix I). The defining slit was made rectangular, 0.2582 ± 0.0005 cm $\times 0.1036\pm0.0005$. The length, R, was 15.40 ± 0.05 cm. Hence $\Delta\Omega$ was $1.128\pm0.015\times10^{-4}$ steradian. The defining slit also determined the angular resolution[10] ($2\Delta\alpha$ in the notation of Appendix I). With foil scattering the resolution was not constant, since the width of foil seen by the counter decreased as $\cos\alpha$ with increasing angle α of the defining counter from the beam. In the worst case (collimator and defining slits horizontal and α small) $2\Delta\alpha \simeq 1.8°$. In general it was considerably less. Both slits were vertical for all the proton-defined data ($2\Delta\alpha \simeq 0.8°$). The conjugate slit was rectangular (1.01

[10] A small error was caused by the finite slit width at certain angles where the cross section was changing rapidly. At angles $\alpha=\alpha^*$, where the effect was not negligible, a small correction (usually about 1 percent) was applied by multiplying by the ratio $n(\alpha^*)2\Delta\alpha/\int_{\alpha^*-\Delta\alpha}^{\alpha^*+\Delta\alpha} n(\alpha)d\alpha$. The correction was required only in the region of small angles so $n(\alpha)$ was given the Rutherford form.

cm×0.85 cm) and 10.08 cm from the foil. All other slits in front of the two counters were merely baffles to shield the counters from collimator slit scattering.

As the counter walls were at high potential, the counters had to be supported on plastic insulators. Likewise, gas leads to the counters, introduced through the rotary joint at the bottom, were broken and joined by plastic sleeves with O-ring vacuum joints.

The two counters had to be capable of independent rotation about the cylindrical axis of the chamber. In the present design this rotation was achieved by means of two concentric brass shafts passing through the bronze bushing in the hub at the bottom of the chamber. An arm was attached to the top of each shaft and a brass block containing the slits and supporting the counter was seated on each arm. Vacuum seals where the shafts passed through the bushing were made with O-rings. These were quite satisfactory. A five-inch gear wheel and a calibrated angle scale were mounted on each shaft. Angles could be read to 0.1° by the scales and verniers.

G. Foil Holder

A 0.75-inch diameter solid brass rod passed through the center of the lid of the chamber. An O-ring seal in the lid allowed the rod to slide and rotate freely without influencing the vacuum. Foils were attached by clear Glyptal to a 2-inch×2-inch brass frame mounted on the lower end of the rod. The foil holder was calibrated for vertical positioning and orientation with respect to the beam direction. While this defined an area vastly greater than was actually traversed by the beam, it was desirable to keep the frame itself as far from the path of the beam as possible.

H. Normalizing Counter Unit

The counters shown in Fig. 2 mounted on the chamber lid were intended to provide a normalizing count to be used as a supplement to the current collector as a measure of the incident particle flux. Probably because of unsuitable design of the counters themselves, leading to poor pulse-height characteristics, this arrangement was not actually used for any of the data reported in this paper.

I. Vacuum System

The chamber was evacuated by a Distillation Products oil diffusion pump backed by a Duo Seal mechanical pump. During operation the gate valve in the slit system was open, and the scattering chamber was directly connected to the main vacuum of the cyclotron. The operating pressure was 10^{-4} mm Hg. The counters were pumped by opening them to the main vacuum of the chamber. Design of the vacuum system of this chamber owed much to the versatility of O-ring seals.[11]

[11] An excellent description of O-ring seals was given by F. N. D. Kurie, Rev. Sci. Instr. **19**, 485 (1948).

J. Checking and Alignment of the Scattering Chamber

Numerous checks were made on the accuracy of machining and assembly of the equipment, but the following were the most significant. A mandril was turned so that one end fitted the ports for the collimator and current collector and the other end fitted the blocks in which the counter slit systems were inserted. Each counter arm was swung round in turn to align with the collimator port and the mandril pushed through the port into the slit block. For this operation to be possible the slit block had to be at the correct height. At the same time the angle scale for that counter was set at 180.0°. The same procedure was repeated at the current collector port. If the collimator and current collector ports were diametrically opposite, the angle scales should then have read zero. Satisfactory checks were obtained (±0.05°).

The chamber was aligned by centering the fluorescent spot caused by the impact of the deuteron beam on the painted glass plate of the current collector. Centering was facilitated by placing a cap with a 0.25-inch central hole over the end of the current collector and centering with respect to the hole. The alignment was done remotely with a mirror and telescope system. Centering was probably correct to within 0.03 inch at the end of the current collector, which corresponded to 0.015 inch at the foil. Vertical alignment was somewhat more critical than horizontal. A vertical error could cause some of the conjugate paths to lie too high or too low for acceptance by the conjugate slit.

K. Electronic Equipment

The counters were connected to preamplifiers which, during operation, sat directly under the scattering chamber to permit short leads. The preamplifiers were connected by 150 feet of coaxial cable stretching from the cyclotron pit to the control room in which the main linear amplifiers, discriminators, coincidence circuit, and scalers were located. Figure 4 is a block diagram of the electronic equipment. Design of the preamplifier

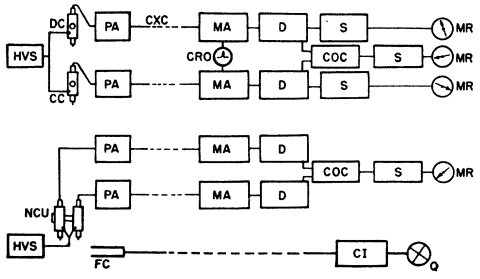

FIG. 4. Block diagram of basic electronic equipment. Abbreviations are as follows: DC-defining counter, CC-conjugate counter, NCU-normalizing counter unit, HVS-high voltage supply, PA-preamplifier, CXC-150 feet of coaxial cable, MA-main linear amplifier, D-discriminator, S-scaler, MR-mechanical register, CRO-cathode-ray oscilloscope, COC-coincidence circuit, FC-Faraday cup, CI-current integrator, Q-quadrant electrometer.

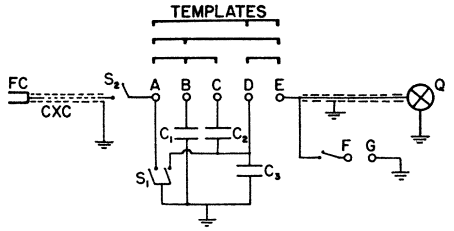

FIG. 5. Current integrator circuit. Connecting terminals ABCDE with the various templates shown above, resulted in different rates of deflection. Nominal values of the condensers were $C_1=1$ μf, $C_2=0.01$ μf, and $C_3=0.1$ μf. When the electrometer was calibrated, the potentiometer was applied at FG. S_1 and S_2 were switches. All switch contacts were platinum to avoid contact potentials. FC-Faraday cup, Q-quadrant electrometer, and CXC-coaxial cable.

and amplifier was due to Elmore, coincidence circuit to Sands, and discriminator and scale of 64 to Higginbotham.

During a run the amplifier operation was monitored with an oscilloscope. Normal cyclotron operation caused no electrical disturbances, whereas faulty operation such as parasitic oscillations were picked up by the amplifiers. The electronic equipment was checked daily by connecting a pulser to the preamplifiers. The output of the amplifiers was checked with a synchroscope. In this way a change in the amplification could be detected. The scalers and coincidence circuit were checked by comparison of the number of counts recorded by each scaler when operated simultaneously. All three scalers should give the same result. The dead time and resolving time of the circuit were measured with a sliding pulser (see Sec. VIII). The resolving time was also measured by placing the counters at an "off coincidence" position; that is, Θ_1 and Θ_2 were not corresponding angles for a 2:1 mass ratio and were sufficiently far from being so that any coincidences observed were the result of chance.[12] The resolving time was computed from $n=2n_1n_2\tau$, where n was the accidental coincidence rate observed, n_1 and n_2 the individual counting rates, and τ the resolving time. τ was $\sim 3\times 10^{-6}$ sec.

V. PROCEDURE FOR OBTAINING SCATTERING DATA

The following procedure was adopted at each pair of angles studied. The counters were set at the calculated angular positions (Sec. III). The cyclotron beam current was adjusted to give a reasonable counting rate in both counters. The optimum discriminator setting was located. This consisted in measuring the number of coincidences as the discriminator bias was raised. The number of coincidences fell off sharply when the bias setting exceeded a certain value. If raising the bias did not alter the coincidence rate, it could be assumed that all the scattering events were being recorded. This check was made on both counters at every angle. When a discriminator check was obtained, the discriminator was advanced as far as had been found to be safe, in order to reduce accidental coincidences to a minimum.

At certain angles, in particular those at which the particles had maximum energy, the discriminator check could not be obtained, owing to the fact that some of the pulses had too nearly the background height. The situation was eased by placing aluminum foils in front of the counter to slow the particles and increase their pulse heights so that a discriminator check could be obtained. Actually, doubts sometimes existed regarding the interpretation of the results obtained with slowing foils. It was found that as the thickness of aluminum increased the number of coincidences first increased but then decreased. This behavior was interpreted as caused by scattering from the slowing foil. Hence, unless a number of different thicknesses of aluminum were tested at each angle and a flat plateau established, there was no guarantee that the maximum coincidence rate observed corresponded to counting of all the scattered particles. Unfortunately, to insert a variety of foils was very time-consuming with the present design because the chamber had to be opened each time a change was made.

The correct angular position of the conjugate counter corresponding to a selected setting of the defining counter was always found by rotating it through several degrees on each side of the calculated conjugate position and recording the coincidence rates. Besides locating accurately the conjugate position, this procedure provided a valuable check on the conjugate beam width. If the slit width was more than sufficient to accept all the particles, the peak was flat; if the peak was sharp, the slit width was too small.

The setting of the conjugate counter having been established, long runs were made to obtain good counting statistics. This was done on each of several foil positions (see Sec. VII) to average over irregularities in the foil. The number of counts obtained at each angle varied from 1000 to 10,000.

VI. CHARGE MEASUREMENT

The charge collected during each run had to be measured for two reasons: (a) successive runs were normalized according to the charge collected during

TABLE I. Capacitance values.

Nominal capacitance	Current	Apparent capacitance
0.1 μf	9.65×10^{-10} amp	0.1057 μf
	1.271×10^{-11}	0.1075
1.0	1.021×10^{-9}	1.122
	4.000×10^{-9}	1.100

Final voltage = 0.850 percent
Limit of error = ±0.5 percent
Short discharge time error = −2 percent

[12] There are processes by which true coincidences could be obtained under such conditions, e.g., as a result of products of nuclear reactions occurring in the foil; but these have negligible probability by comparison with the chance rate.

each; (b) to calculate absolute cross sections it was necessary to know the total number of particles traversing the chamber. The beam current through the chamber was actually about 10^{-8} to 10^{-9} amp.

The Faraday cup of the current collector was connected by coaxial cable to a network of three condensers, whose nominal capacitances were $C_1=1.0$, $C_2=0.01$, and $C_3=0.1$ μf, arranged as in Fig. 5. The capacitances of these condensers were measured by the Bureau of Standards under conditions as nearly as possible resembling those used in the actual scattering operations. These conditions were that the condensers were charged to a potential of 0.8 volt in an interval ranging from 200 to 900 seconds. The capacitances reported differed appreciably from the labeled values, and were subject to even further correction if discharge times of less than 15 minutes were employed. The values are listed in Table I.

The potential developed was applied to a calibrated Compton electrometer. Operation of the integrator comprised the following steps: (a) Faraday cup grounded by closing switch S_1, and the electrometer brought to zero, (b) switch S_2 closed to connect cup to network, (c) S_1 opened allowing integration to commence, (d) at the end of run S_2 opened, stopping integration. The electrometer reading was then noted. Operation of S_1 and S_2 automatically turned the scalers on and off simultaneously. The electrometer was calibrated at regular intervals by means of a Leeds and Northrup potentiometer standardized against a Weston cell calibrated by the Bureau of Standards.

Several sources of error had to be reckoned with such as (1) leakage of charge from the integrator system, cable, etc. This was measured by charging the system to a definite potential and observing the change in deflection of the electrometer as a function of time after the source of potential was removed. The leakage resistance, R, was calculated from $V=V_0\exp(t/RC)$. It varied slightly with the seasons but kept within the range 5×10^{10} to 10^{11} ohms. The correction for leakage was applied to observed electrometer deflections as follows:

$$D_{\text{true}}=D_{\text{obs}}(1+T/2RC),$$

where T was the total running time. The correction rarely exceeded two percent. No variation of leakage rate was observed when the cyclotron was operating. (2) The capacitance of the 150 feet of coaxial line was appreciable when the charge was applied to the 0.1-μfd condenser. It amounted to ~10 $\mu\mu$f per foot, and hence the total capacitance was 0.0015 μf. This capacitance was included in the calculation of total charge collected. (3) Production of secondary electrons in the Faraday cup was guarded against by providing a magnetic field across the current collector. (4) Ionization currents in the residual air in the collector were negligible at the operating pressures used and with 10-Mev particles. (5) To determine whether the neutron and gamma-ray flux in the cyclotron room affected the rate of integration of charge, the gate valve in the slit system was closed and the electrometer connected. No measurable deflection was detected when the cyclotron was turned on.

Charge measurement errors from all sources during the April run were believed to be $\lesssim0.5$ percent.

VII. SCATTERING FOILS

To satisfy the requirements of the experiment it was only necessary to use as scattering material any hydrogenous foil. To reduce the relative accidental coincidence rate it was desirable to choose a material having a high proton content. Nylon ($C_{12}H_{22}N_2O_2$), 0.2 mil thick, was used in the September run (H content ~10 percent). Nylon suffered from two defects. (1) It stretched too readily. In order for a smooth foil to be obtained, stuck to the holder, the Nylon had to be stretched taut by hand. It was difficult to keep the foils uniformly thick over the 2-inch by 2-inch holder. Each foil was examined by means of a Michelson interferometer, and only those foils whose interference patterns seemed satisfactory were used; but the accuracy of this control was not high. (2) Nylon foils changed their characteristics considerably under bombardment, confirming the experience of R. R. Wilson *et al.*[1]

During the December and April runs, 0.25-mil p.e.t. foils were substituted. Du Pont gave the formula $C_{10}O_4H_8$, corresponding to a hydrogen content of greater than 4 percent. However, p.e.t. proved far superior in spite of its lower hydrogen content.

After completion of each scattering run an accurately known area of each foil was removed (18.90 cm^2), weighed on a microbalance, and analyzed for hydrogen. Foils were stored in vacuum until analyzed. Analyses were carried out by burning in dry oxygen and weighing the water of combustion. The number of H atoms per cm^2 was obtained by substitution in the equation, $N_a=fmN/sA$, where m was the mass of the scattering foil, f, its fraction H content, N, Avogadro's number (6.025×10^{23}), s, the area of foil, and A, the atomic weight of H (1.0081). Resulting N_a values used in the calculations of cross sections were as follows:

December 1948,
Foil 3: $(1.86\pm0.09)\times10^{19}$ H atoms cm^{-2}
April 1949, Foil 4: $(1.41\pm0.07)\times10^{19}$
Foil 5: $(1.68\pm0.08)\times10^{19}$.

The September foils were not analyzed. The large errors quoted were contributed almost wholly by uncertainty in f (±4 or 5 percent). The value of m may be ±0.025 percent in error and of s about ±0.1 percent. Moreover, it should be realized that the actual error may be even larger than this. These errors do not include (a) non-uniformity of the foil. Scattering was measured only from the area of foil actually traversed by the beam in the course of a run, comprising about

1 percent of the whole area of the foil, whereas N_a values were derived from the entire foil. Some idea of the importance of this circumstance was conveyed by the fact that the counting rate varied from one position to another by as much as 10 percent. (b) Foil change under bombardment. This was eliminated as completely as possible by using certain areas of the foil infrequently, thereby preserving them as "standards" with which the more bombarded areas of the foil could be compared from time to time. This procedure guarded against errors in relative cross sections at different angles due to any progressive foil change.

VIII. CORRECTIONS ARISING FROM COINCIDENCE CIRCUIT

A. Accidental Background

Individual counters responded to deuterons scattered by the carbon and oxygen present in the foil. Hence, the individual counting rates were much greater than the coincidence rate. By chance it was possible for two particles not related to the same nuclear collision to activate the two counters during a time interval less than the resolving time of the coincidence circuit. A coincidence was then recorded. When data was taken, the total number of counts recorded in each counter was noted, n_1 and n_2 respectively, as well as the number of coincidences. The resolving time of the coincidence circuit, τ, which was about 3×10^{-6} sec, and the total running time T being known, the number of chance coincidences, n', was calculated from the formula $n'=2n_1n_2\tau/T$ and was subtracted from the observed number of coincidences, n_c. Accidentals rarely exceeded a few percent.

B. Dead Time of Coincidence Circuit

A certain fraction of true coincidences was lost because the coincidence circuit was inoperative for an interval, τ', following each count ($\tau'=26\times10^{-6}$ sec). Any further counts arriving before the circuit had recovered could not be recorded. This meant that during a running time, T, the coincidence circuit was dead for a time $(n_1+n_2)\tau'$, leading to an additive correction of the type $n''=n_c(n_1+n_2)\tau'/T$, where n'' was the number of coincidences lost which were to be added to the number actually recorded, n_c. This correction amounted to several percent at some angles. Both of the above corrections involved T^{-1}. Therefore, both corrections were diminished relative to true coincidences by using small beam currents and slow counting rates. On the other hand, longer times increased the electrometer leakage correction. Owing to the prolific scattering of deuterons from C and O at small angles, corrections for both accidentals and dead time were always worst there. It was preferable to use the defining counter with its much smaller aperture at the smaller angle of the conjugate pair; e.g., near $\Theta_1=17.9°$,

TABLE II. Complete tabulation of differential cross section measurements. Cross sections, $\sigma(\theta)$, and angles, θ, refer to center-of-mass coordinates. Data from five foils are listed separately. Laboratory angle pairs, Θ_1 and Θ_2, are included. Uncertainties after each measurement are standard deviations based on the number of coincidences. Symbols at the head of each column of cross sections are used to represent the column in Fig. 6. The next-to-last column lists average $\sigma(\theta)$ values. The last column lists some ratios of observed to Rutherford-Darwin cross sections.

Run			September 1948*		December 1948		April 1949			
Foil number			1	2	3	4	4	5	Weighted	
Defining			Deut.	Deut.	Deut.	Deut.	Prot.	Deut.	average	
Scattering foil			Nylon	Nylon	P.e.t.	P.e.t.	P.e.t.	P.e.t.	$\sigma^a(\theta)$	
Symbol (Fig. 6)			×	●	△	⊡	⊙	+	$\times10^{25}$	$\frac{\sigma(\theta)_{av.}}{\sigma(\theta)_{R-D}}$
Θ_1	Θ_2	θ			$\sigma(\theta)\times10^{25}$ cm² steradian^{-1}				b	
14.63	67.5	45			1.75±0.02 c	1.51±0.02 m		1.59±0.02 m	1.79	
16.17	65.0	50			1.71±0.02				1.66	45
17.65	62.5	55				1.43±0.02		1.52±0.02	1.56	
19.10	60.0	60			1.48±0.01		1.51±0.04		1.44	
20.52	57.5	65					1.37±0.03		1.32	
21.87	55.0	70	1.12±0.02	1.13±0.03	1.21±0.01		1.19±0.03		1.21	110
23.15	52.5	75				1.06±0.01	1.11±0.02	1.08±0.01	1.10	
24.37	50.0	80	0.99±0.02	0.92±0.02	0.98±0.01		1.03±0.02		0.99	
25.52	47.5	85					0.94±0.02		0.89	
26.57	45.0	90	0.78±0.02	0.77±0.01	0.77±0.01		0.82±0.02		0.79	170
27.50	42.5	95					0.79±0.02		0.71	
28.33	40.0	100	0.63±0.02	0.65±0.01		0.61±0.01	0.71±0.02		0.63	
29.02	37.5	105		0.58±0.01		0.59±0.01	0.61±0.02		0.59	
29.53	35.0	110					0.59±0.01		0.57	220
29.88	32.5	115					0.60±0.02 d		0.57	
30.00	30.0	120					0.63±0.02 d		0.61	
29.87	27.5	125					0.69±0.02 d		0.68	
29.43	25.0	130				0.75±0.01	0.80±0.02		0.79	450
28.67	22.5	135		1.03±0.02		0.91±0.02	0.98±0.02		0.97	
27.52	20.0	140	1.06±0.05	1.26±0.02		1.17±0.02	1.23±0.02		1.22	
25.92	17.5	145		1.50±0.04		1.60±0.04	1.43±0.03		1.47	
23.78	15.0	150		1.87±0.04		1.92±0.05	1.75±0.03		1.79	1300
21.13	12.5	155				2.24±0.22	2.09±0.03		2.12	
17.87	10.0	160					2.40±0.03 m		2.43	1900

[a] Relative values only.

[b] Final results of experiment.

$\Theta_2 = 10.0°$ defining the protons at Θ_2 was more suitable, whereas near $\Theta_1 = 16.2°$, $\Theta_2 = 65.0°$, it was somewhat preferable to define the deuterons at Θ_1.

Another factor contributing to the individual counting rates was the neutron and gamma-ray background in the cyclotron room (the neutrons presumably coming from (dn) and $(d,2n)$ reactions[13] on the copper dees and target plate). For the same coincidence rate the individual counting rates were noted to vary haphazardly. This effect was reduced during the April run when the equipment was surrounded by a 16-inch concrete wall.

IX. MEASUREMENT OF BEAM ENERGY

The mean energy of the beam and its half-width at the end of the slit system were obtained by measuring lengths of deuteron tracks in Ilford C2 Nuclear Research Emulsions. A convenient number of tracks was obtained by scattering the deuterons from 0.1-mil platinum foil through an angle of 20°. Deuterons entered the emulsions at ~3°, and track lengths were measured with a Leitz microscope and calibrated eyepiece micrometer. A check on the range-energy curve for C2 emulsions was made by measuring tracks of UI and UII in a plate from the same batch loaded with uranium. This checked the curve only at much lower energies but was useful in verifying that the emulsions did not change their characteristics appreciably. The range-energy curve published by Lattes *et al.*[14] formed the basis of the energy measurements.

Two independent measurements of the beam energy were made by the photographic method. Mean ranges of the deuterons, after correction, corresponded to 9.95±0.10 Mev and 9.85±0.10 Mev respectively. Corrections were made for loss of energy in traversing the Pt foil and energy transferred to the Pt nucleus in elastic collision. An independent check was made by Mr. J. Miskel, who measured the activation of Al foils behind various thicknesses of Al absorber. This gave 10.1±0.2 Mev. Plates exposed in the photographic scattering chamber yielded 10.1±0.1 Mev. This range of variation was well within the uncertainty of the range-energy relationship for the emulsion. However, as no attempt to control the beam energy was made during the course of the runs, each of which extended over several weeks, it probably varied slightly with the deflector voltage and exact location of the arc structure.

The stopping power relative to air of the p.e.t. foil was calculated to be 1000. Scattering foils were $\sim 6\times10^{-4}$ cm thick, corresponding to a mean energy loss before collision (half-thickness) of about 30 kev. This correction was negligible. The beam energy to which the present data correspond may conservatively be taken as 10.0±0.2 Mev. The half-width of beam energy distribution after correction for straggling in the emulsion was approximately 70 kev.

[13] J. C. Grosskreutz, Phys. Rev. **76**, 482 (1949).
[14] Lattes, Fowler, and Cuer, Proc. Phys. Soc. London **59**, 883 (1947).

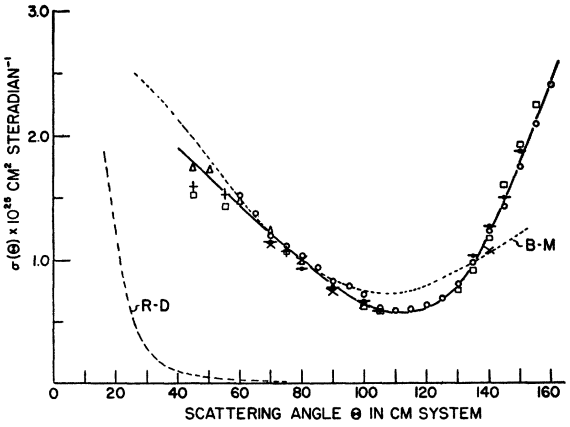

FIG. 6. Differential d-p cross sections in the center-of-mass system, in units of 10^{-25} cm² steradian^{-1}. All values listed in Table II are plotted with the symbols of Table II. The smooth curve is considered to be the best fit to the data after the worth of each point is estimated. The dotted curve *R–D* was calculated from the Rutherford-Darwin formula and the dotted curve *B–M* is based on data supplied by Buckingham and Massey (theoretical).

The purity of the deuteron beam was checked by setting the counter at 90° with respect to each other and then measuring the coincidence rate. It was no greater than the usual background rate, indicating that there were no appreciable number of protons in the beam (<1 percent).

X. REDUCTION OF DATA

If $\sigma(\alpha)$ is the cross section in the laboratory for scattering (or recoil) into unit solid angle at angle α (measured from the incident beam), N_i, the number of incident particles, N_a, the number of scattering centers per cm², $n(\alpha)$, the number of scattered (or recoil) particles entering the defining counter, and $\Delta\Omega$, the solid angle subtended by the defining slit at the center of the foil, then

$$\sigma(\alpha) = n(\alpha)/N_a N_i \Delta\Omega.$$

When defining deuterons, $\alpha = \Theta_1$, and when defining protons, $\alpha = \Theta_2$. For any one electrometer deflection, to obtain $\sigma(\alpha)$ it was necessary to know $n(\alpha)$, N_i, N_a, and $\Delta\Omega$. Determination of each of these has been described in previous sections.

Conversion to Center of Mass

The data obtained were reduced from laboratory coordinates to a center-of-mass (CM) coordinate system as follows:

(a) Defining deuterons: if $\sigma(\Theta_1)$ is the measured cross section in the laboratory, then $\sigma(\theta)$, the cross section in CM, relates to the angle of scattering, Θ_1, in the laboratory and θ in CM as follows:

$$\sigma(\theta) = \sigma(\Theta_1)(\sin\Theta_1/\sin\theta)^2 \cos(\theta - \Theta_1).$$

The angles are related by $\theta = \pi - 2\Theta_2$.

(b) Defining protons: if $\sigma(\Theta_2)$ is the cross section in the laboratory, then

$$\sigma(\theta)=\tfrac{1}{2}\sigma(\Theta_2)(\sin\Theta_2/\sin\theta).$$

The kinetic energy in the *CM* system associated with the relative motion of scattered and recoil nuclei is given by

$$E_0'=m_2E_0/(m_1+m_2)=1/3E_0=3.3 \text{ Mev},$$

where E_0 is the kinetic energy of the incident deuterons in the laboratory.

XI. RESULTS AND DISCUSSION

Table II summarizes the experimental results on the angular dependence of *d-p* cross sections. Values are given for the five foils studied during the three runs. Only three points were taken on Foil 5, enough to give an additional check on absolute cross sections. Owing to accidental loss of Foils 1 and 2 before the chemical analysis had been carried out, only relative values were obtained from the September run. The absolute values quoted were obtained by fitting the data to the December and April runs.

All data are shown in Fig. 6 as $\sigma(\theta)$ *versus* θ. The smooth curve is considered to be the best fit. Table II also includes average values for $\sigma(\theta)$ as read from the smooth curve. Values marked "*m*" in Table II were open to suspicion because of multiple scattering and should be treated as lower limits. Values "*c*" were corrected for multiple scattering, corrections being based on the data obtained when the scattering foil was rotated (see Appendix II). At these angles some loss may have occurred because of failure of some protons to penetrate the conjugate counter window. A similar situation occurred for the deuterons at $\theta=160°$ in the proton-defined data. Here $E_1=1.4$ Mev, corresponding to a range in air of 2.7 cm. The air equivalent of the longest path through the scattering foil plus the conjugate window was 1.2 cm, and allowance also had to be made for range straggling within the window itself. Even so, window effects were small at these angles, and these were the worst cases.

Between $\theta=115°$ and 125° (indicated by "*d*" in Table II) cross sections were too high owing to "double counting" and should be regarded as upper limits. This "double counting" refers to the fact that when both counters were near 30° in the laboratory system, besides the *bona fide* coincidences from protons entering the defining counter and deuterons entering the conjugate counter, it was possible to record some spurious coincidences from deuterons entering the defining counter and protons entering the conjugate counter.

The limits of error given after each value in Table II are standard deviations based solely on the number of coincidences contributing to the value. They should be regarded as lower limits to the actual errors. Taking account of all sources of uncertainty, the extreme limits of error are considered to lie within ±3.5 percent for the relative cross sections and ±5 percent for the absolute cross sections. However, it must be remarked that in any experiment as complex as this, small systematic errors can easily remain concealed.

As a matter of general interest some Rutherford-Darwin cross sections have been computed and are included in Fig. 6 (dotted curve *R–D*). The ratio of experimental to *R–D* cross sections has been tabulated in the last column of Table II for certain angles. The magnitude of these is of interest merely to emphasize the dominance of specifically nuclear forces at this energy.

The most extensive theoretical treatment[15] of *n-d* and *p-d* scattering is the work of Buckingham and Massey. They assumed an interaction energy between the nucleons,

$$V(r)=A(mM+hH+bMH+w)e^{-2r/a}.$$

M is the Majorana operator, H the Heisenberg operator; various assumptions were made concerning the constants *mhbw*, and cross sections derived in each case. Comparison of these cross sections with experiment has been made in three ways. (a) Total *n-d* cross sections at a variety of energies. (b) Differential *n-d* cross sections. Both of these strongly support exchange type (symmetrical) rather than ordinary (neutral) forces. (c) Differential *p-d* cross sections. Here comparison has previously been made[16] for a proton energy of 1.85 Mev. Cross sections based on ordinary forces were too large at all angles by a large factor (~60 percent) while exchange forces showed reasonable agreement over most angles, being somewhat too small at large angles, e.g., by about 20 percent at $\theta=150°$.

The present results, corresponding to 5-Mev *p-d* scattering, are of special interest at large angles. The Buckingham and Massey 5-Mev data are included in Fig. 6 (dotted curve *B–M*). Agreement between experimental and theoretical values is remarkably good for $\theta\lesssim 90°$, but thereafter the theoretical curve is too shallow; e.g., at $\theta=150°$ the discrepancy is around 33 percent and increases rapidly with angle. The steep rise in cross sections beyond $\theta=120°$ has been confirmed[17] and now appears to present a new aspect of the *p-d* interaction.

On quite general grounds one might expect anomalies to develop at large angles (presumably associated with small approach parameters). It is not obvious at present whether the large angle anomaly arises solely from neglect, in the theory, of polarization of the deuteron or indicates that even the extremely general potential

[15] For the *n-d* case see R. A. Buckingham and H. S. W. Massey, Proc. Roy. Soc. **A 179**, 133 (1941); Phys. Rev. **71**, 558 (1947). Treatment of the *p-d* interaction along the same lines has been completed recently. We are indebted to Professor Massey for sending us theoretical cross sections in advance of publication.

[16] H. S. W. Massey and R. A. Buckingham, Phys. Rev. **73**, 260 (1948).

[17] Communication from Los Alamos Scientific Laboratory, Los Alamos, N. M.; also confirmatory work in this laboratory using a photographic scattering chamber.

assumed by Buckingham and Massey is inadequate, in which case the cause of the anomaly may be fundamental. One would expect polarization effects to vanish at sufficiently high energy, whereas the discrepancy evidently increases with energy.

It is a pleasure to acknowledge the interest of Professors R. N. Varney and A. L. Hughes in the progress of the experiment. The excellent performance of the mechanical equipment reflects the skill of Mr. O. Retzloff and his workshop staff. We wish to thank the crew of the cyclotron under Mr. A. A. Schulke for co-operation throughout, Mr. J. C. Grosskreutz who worked with us on the beam energy determinations, Du Pont de Nemours for providing the foil materials, Miss Dorothy Kuene of the Chemistry Department for analyzing the foils, and Mr. P. Bohlman who assisted in the taking of data. One of us (KBM) acknowledges his Studentship from Science and Industry Endowment Fund, Commonwealth of Australia.

APPENDIX I. CALCULATION OF GEOMETRICAL CONJUGATE PATTERN

A. Height

Figure 7 is a projection on a plane perpendicular to the beam of paths of scattered and recoil particles. Here a is the vertical height of beam where it strikes the foil, h_1, the height of the defining slit, h_2, the height of the geometrical conjugate pattern (g.c.p.) corresponding to h_1, L_1, the distance between center of scattering foil and defining slit, L_2, the distance between scattering foil and conjugate slit, α, the angle at which the defining counter is set, and β, the conjugate angle. The incident beam, path of the scattered particle, and path of the recoil particle must be coplanar. Extreme paths of scattered and recoil particles are shown in Fig. 7. These determine the height of the g.c.p., h_2.

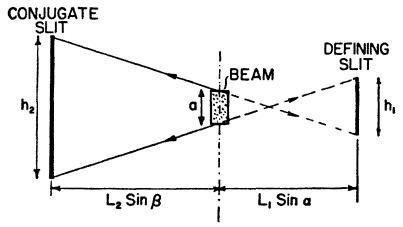

FIG. 7. Relationship between heights of defining and conjugate slits. Extreme paths of particles scattered from the top and bottom of the beam are illustrated.

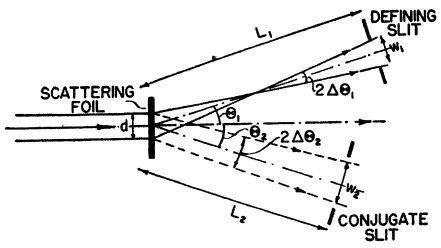

FIG. 8. Relationship between width of defining and conjugate slits. Extreme paths of deuterons entering the defining slit and recoil protons entering the conjugate slit are shown for the case $\Theta_2<30°$. Extreme rays for other cases were similar but not identical.

It follows from the geometry that

$$h_2=a+(h_1+a)L_2\sin\beta/L_1\sin\alpha.$$

In the present experiment $L_2/L_1=0.65$. When defining deuterons, $\alpha=\Theta_1$, $\beta=\Theta_2$. When defining protons, $\alpha=\Theta_2$, $\beta=\Theta_1$.

B. Width

Figure 8 is a projection on a horizontal plane of extreme paths of scattered and recoil particles. Here, also, it is necessary to distinguish between deuteron definition and proton definition. It is also necessary to distinguish the treatment for $\Theta_2<30°$ and $\Theta_2>30°$. Figure 8 applies to deuteron definition, $\alpha=\Theta_1$, $\beta=\Theta_2$, when $\Theta_2<30°$. The treatment is similar for the other cases, but not identical. w_1 is the width of the defining slit, w_2, the corresponding width of the g.c.p., and d, the width of the beam where it strikes the foil. $2\Delta\Theta_1$ is the angle between extreme rays entering the defining slit (corresponding to angles $\Theta_1^*=\Theta_1+\Delta\Theta_1$ and $\Theta_1^{**}=\Theta_1-\Delta\Theta_1$), and $2\Delta\Theta_2$ is the angle between corresponding recoil protons, i.e., $\Theta_2^*-\Theta_2^{**}$. To compute w_2 from w_1, the procedure is as follows: obtain $\Delta\Theta_1=(w_1+d\cos\Theta_1)/2L_1$, then calculate Θ_2^* and Θ_2^{**} corresponding to Θ_1^* and Θ_1^{**} using $\sin(2\Theta_2+\Theta_1)/\sin\Theta_1=2$, and hence get $2\Delta\Theta_2$, and then compute $w_2=(d\cos\Theta_2+L_2 2\Delta\Theta_2)$. It is possible to obtain w_2 explicitly, but the above proved to be more convenient.

It has been assumed in the above that the deuterons traversing the chamber were all perfectly collimated. The presence of small transverse components would increase the width of the g.c.p. slightly.

APPENDIX II. MULTIPLE SCATTERING

Figure 9 represents the scattering process occurring within the foil. Deuterons have full energy from A to B and reduced energy after collision from B to C. Protons recoil along BD. Multiple scattering occurs along AB, BC, and BD; and the effect is to spread the cones of scattered and recoil particles. The spread at C and D may be represented by a Gaussian distribution. Suppose that deuterons are being defined. Coincidences can be lost by (1) deuterons being multiply scattered so as to miss the defining slit. This is most probable where the deuterons have low energy. The order of magnitude of this effect can be found by calculating the rms angle of scattering using Williams' formula.[18] The probability that a particle undergoes a resultant deflection ϕ (projected deflection on a plane) into an angular range $d\phi$ is

$$P(\phi)d\phi=(2/\pi\cdot\langle\bar{\phi}^2\rangle)^{\frac{1}{2}}\exp[-\phi^2/2\langle\bar{\phi}^2\rangle]\cdot d\phi,$$

where $\langle\bar{\phi}^2\rangle$ is the mean square angle of scattering,

$$\langle\bar{\phi}^2\rangle=\frac{\pi}{2}\left(\frac{Ze^2}{E}\right)^2 N_v\frac{4}{9}t\ln\left[\frac{Z^{4/3}N_v t\hbar^2 M}{4\pi m^2 E}\right],$$

and Z is the mean atomic number of the foil. For p.e.t. $Z_{av.}\simeq 4.5$, e is the electronic charge, E, the energy of the particle, N_v, the number of nuclei per $cm^3=N\rho\nu/\bar{M}$, where N is Avogadro's number, $\bar{M}$, the gram-molecular weight of p.e.t.$=192$, ρ, the density of p.e.t.~ 1.1 g cm^{-3}, and ν, the number of nuclei per molecule$=22$, whence $N_v\simeq 7.6\times 10^{22}$. t is the maximum path

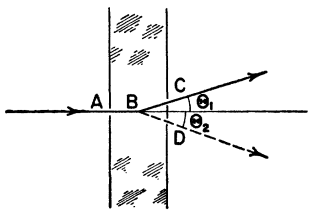

FIG. 9. Scattering within a foil. Deuteron enters at A and collides at B. Deuteron leaves at C and proton at D.

[18] E. J. Williams, Proc. Roy. Soc. **A 169**, 521 (1938); Phys. Rev. **58**, 292 (1940); Revs. Modern. Phys. **17**, 217 (1945).

length[19] and $\frac{4}{9}\cdot t$ the effective path length. The foil was ~0.25 mil. h is Planck's constant, M, the mass of the deuteron, and m, the mass of the electron. The combined rms value $\langle\bar{\phi}^2\rangle^{\frac{1}{2}}$ due to AB and BC must be calculated assuming the foil to be normal to the incident beam. For AB, $E_0=10$ Mev, and $\langle\bar{\phi}^2\rangle^{\frac{1}{2}}\simeq 0.048°$, which is negligible. For BC, ($\Theta_1=21.1°$, $\Theta_2=12.5°$), $E_1\simeq 1.5$ Mev, $\langle\bar{\phi}^2\rangle^{\frac{1}{2}}\simeq 0.39$. The angles subtended at the foil by the defining slit were 0.38° and 0.95° (vertical and horizontal dimensions respectively); therefore, the rms angle of scattering was comparable in size to the angles subtended by the slit. On this basis a gross loss of counts would be anticipated at this angle. However, there was a compensating mechanism. Deuterons which would have just missed the defining slit can be multiply scattered into it and will cause a coincidence if their conjugate protons can also enter the conjugate slit. Effectiveness of compensation, therefore, depends on conjugate slit size. We can estimate how much it needs to be increased beyond the g.c.p. to provide practically complete compensation by calculating the conjugate angle $\delta\Theta_2$ corresponding to $\langle\bar{\phi}^2\rangle^{\frac{1}{2}}$. At $\Theta_2=12.5°$, $\partial\Theta_2/\partial\Theta_1\sim 1$, therefore, $\delta\Theta_2\simeq 0.39$; $L_2=10.1$ cm, hence $\delta w_2\simeq 0.07$ cm. Similarly, $\partial h_2/\partial h_1\simeq 0.4$, $\delta h_1\simeq 0.1$ cm, whence $\delta h_2\simeq 0.04$ cm; i.e., a margin of ~0.07 cm at each side and ~0.04 cm at top and bottom are required to compensate for rms scattering. The g.c.p. at this angle is height 0.46 cm and width 0.28 cm. The actual size was 1.01 cm×0.85 cm, so there was ample margin for complete compensation. Actually, the situation was more complicated because there were several baffles which may have interfered with compensation, and it is almost impossible to estimate their effect. The best criterion for this and similar cases is a comparison of deuteron-defined with proton-defined data for the same angle pair. (2) Coincidences can also be lost by protons being multiply scattered so as to miss the conjugate slit. For this there is no compensating process. It can be prevented only by making the slits sufficiently large to collect effectively all protons in spite of multiple scattering. (Notice that in both (1) and (2) it is the size of the conjugate slit which must be increased because of multiple scattering—in (2) to catch all the proper coincidences and in (1) to catch the necessary compensating coincidences.) When defining deuterons (2) is worst when Θ_2 is large. For $\Theta_2=67.5°$, t is increased 2.6 times, $E_2\simeq 1.3$ Mev, $\langle\bar{\phi}^2\rangle^{\frac{1}{2}}\simeq 0.67°$, whence the g.c.p. must be increased on all sides by a strip 0.12 cm. The required g.c.p. size is 0.66 cm ×0.43 cm. Allowing for non-uniform distribution of particles across the g.c.p., a margin of two "rms distances" would be adequate, requiring the slit to be 1.04 cm×0.91 cm. Evidently some counts were lost at this angle. Moreover, the chamber was certainly not exactly aligned, and there was in any case some uncertainty in the g.c.p. owing to diffuse edges of the beam. It was, therefore, impossible to calculate any meaningful correction. Instead, an experimental check on multiple scattering was made at $\Theta_2=65°$ and 67.5° by rotating the scattering foil away from the normal to the beam in such a direction that the low energy proton could escape more readily. However, at the same time this process rapidly increased the path length of the deuteron ($\Theta_1=14.6°$); and although its energy was 8.6 Mev, its value of $\langle\bar{\phi}^2\rangle^{\frac{1}{2}}$ soon became significant and made excessive demands on the compensating mechanism (especially as regards height of the conjugate slit because of $\partial h_2/\partial h_1$ being 2.4 at this angle). It was indeed observed that the coincidence rate (reduced) initially increased as the foil was rotated, but reached a maximum and then declined with continued rotation, indicating the presence of multiple scattering and confirming the above reasoning. A correction was applied to the data at $\Theta_2=67.5°$ and 65° of the December run based on these observations.

Between about $\Theta_2=25°$ and 35° there is danger of losing coincidences, when defining deuterons, owing to inadequate conjugate slit width ($\partial\Theta_2/\partial\Theta_1\gg 1$). In general we did not take data closer than 22.5° and 37.5° for this reason (both these angles being safe even allowing for spread due to multiple scattering).

Similar considerations apply to proton-defined data; but it is found that multiple scattering losses are less serious here, a difference which is one advantage of defining protons. Width requirements for the conjugate slit are very easily met; but height requirements are worst when Θ_2 is small; e.g., $\Theta_2=10.0°$, $\Theta_1=17.9°$, $E_1=1.4$ Mev. Calculation of $\langle\bar{\phi}^2\rangle^{\frac{1}{2}}$ indicates that some coincidences were probably lost here (of the order of a few percent). At $\Theta_2=12.5°$ there was no loss from multiple scattering.

[19] The factor 4/9 appears with t because particles can have all lengths in the foil from 0 to t with equal probability and the average of $t^{\frac{1}{2}}$ is $\left[\left(\frac{4}{9}\right)t\right]^{\frac{1}{2}}$.

PHYSICAL REVIEW VOLUME 81, NUMBER 1 JANUARY 1, 1951

The (p,n) Reaction on Scandium and Vanadium: Energy Levels of Ti^{46} and Cr^{52}*

W. D. Baker,† J. S. Howell,† Clark Goodman, and W. M. Preston
Laboratory for Nuclear Science and Engineering, Massachusetts Institute of Technology, Cambridge, Massachusetts
(Received August 25, 1950)

Thin targets of the monoisotopic elements vanadium and scandium were bombarded with magnetically resolved protons at energies up to about 4 Mev. The neutron and gamma-ray yields were measured as functions of the proton energy. In each case a number of maxima are observed in the yield curves, presumably corresponding to excited states in the compound nucleus.

I. INTRODUCTION

THE reactions $V^{51}(p,n)Cr^{51}$ and $Sc^{45}(p,n)Ti^{45}$ have been mentioned by Hanson, Taschek, and Williams[1] as useful monoenergetic neutron sources at low energies. As compared with the $Li^7(p,n)$ reaction, the greater weights of V^{51} and Sc^{45} result in a much lower neutron energy at the reaction threshold‡ and a smaller variation of energy with angle in the laboratory frame of reference. In addition, a study of the variation of the neutron yield with energy furnishes information about the energy levels of two medium weight nuclei, Ti^{46} and Cr^{52}, in the excitation range above particle

* This research has been partially supported by a joint program of the ONR, the Bureau of Ships, and the AEC.
† Lieutenant Commander and Lieutenant, U.S.N., respectively. Submitted in partial fulfillment of the requirements for the degree of Master of Science in Physics under the Naval Postgraduate Training Program.
[1] Hanson, Taschek, and Williams, Rev. Modern Phys. **21**, 635 (1949).

‡ The neutron energies at zero degrees and at the (p,n) threshold are 29, 1.37, and 0.57 kev for the $Li^7(p,n)$, $Sc^{45}(p,n)$, and the $V^{51}(p,n)$ reactions, respectively.